PERGAMON

International Journal of Heat and Mass Transfer 45 (2002) 1197–1209

International Journal of HEAT and MASS TRANSFER

www.elsevier.com/locate/ijhmt

On numerical modelling of low-pressure subcooled boiling flows

J.Y. Tu *, G.H. Yeoh

Australian Nuclear Science and Technology Organisation (ANSTO), Private Mail Bag 1, Menai, NSW 2234, Australia

Received 28 November 2000; received in revised form 6 July 2001

Abstract

Although models of subcooled flow boiling at high pressure have been studied extensively, there are few equivalent studies for numerical modelling at low pressure. Recent experimental and numerical studies on subcooled boiling flow at low pressure have indicated that empirical models developed, and verified, for high-pressure situations are not valid at low pressures. A study has been conducted to extend a two-fluid model, previously used for predicting subcooled boiling flow at high pressures into being applicable for low-pressure conditions. This study demonstrates that the following closure relationships or parameters are important for an accurate prediction of void fraction distributions at low pressures: (i) partition of the wall heat flux; (ii) bubble size distribution and interfacial area concentration; and (iii) bubble departure diameter and its relationship with bubble frequency. Different existing correlations for all these are tested and some new correlations are proposed. Predictions of the proposed model agree closely with a number of published experimental data.

1. Introduction

Modelling of a subcooled boiling flow is important in many industrial applications, one of such is the nuclear industry. It is important because an accurate knowledge of the void fraction distribution in reactor cores is required to properly perform various safety analyses. Most available subcooled flow boiling models were developed for and tested at high-pressure conditions typical of power reactors. The present work, however, is driven by the need for analysis of a low-pressure research reactor *HI*gh *F*lux *A*ustralian *R*eactor (HIFAR) at ANSTO and its eventual replacement.

Thus, as demonstrated in Fig. 1, reactor safety analysis codes such as RELAP5 [1] and CATHARE [2], which use such models, cannot satisfactorily predict void fraction distributions in low-pressure subcooled boiling flows [3]. This limitation on the use of the RELAP5 code for low-pressure research reactor application was also reported in [4].

To overcome this limitation, we used a general-purpose computational fluid dynamics (CFD) code, CFX-4.2, to assist us develop subcooled boiling models for low-pressure conditions. However, studies and tests of the subcooled flow boiling model in the CFX code [5] have revealed that it also had been validated only for relatively high-pressure flows. For example, Kurul [6] and Anglart [7] tested a subcooled boiling flow in a pipe, at a pressure of 4.5 MPa. Anglart and Nylund [8] predicted void fraction distributions in one- and six-rod fuel bundles, where they validated the model against experimental data at a range of system pressures near 5.0 MPa. Recently, Mi et al. [9] further developed the CFX subcooled boiling model and validated the model against Bartolomei's [10] high-pressure boiling experiments.

Although the boiling model in the CFX-4.2 code has been satisfactorily validated for subcooled boiling flows at these pressures, the model is not valid for low pressure [11] boiling flow applications. Recent experimental and computational studies reported in literature have indicated that the bubble behaviour determining the void change at low pressure differs significantly from that at

* Corresponding author. Tel.: +61-2-97173138; fax: +61-2-97179263.

E-mail address: tuj@ansto.gov.au (J.Y. Tu).

0017-9310/02/$ - see front matter
PII: S0017-9310(01)00230-7

Nomenclature

A_{lg}	interfacial area concentration
A_q	fraction of wall area subjected to cooling by quenching
Bo	boiling number $= q/Gh_{fg}$
C_D	non-dimensional drag coefficient
C_{pl}	liquid specific heat
D	mean bubble diameter
d_0, d_l	reference bubble diameters
d_{Bw}	bubble departure diameter
D_s	mean Sauter bubble diameter
f	bubble departure frequency
G	mass flux
h_{fg}	latent heat
h_{lg}	inter-phase heat transfer coefficient
Ja	Jakob number $= \rho_l C_{pl}(T_{sat} - T_l)/\rho_g h_{fg}$
m	inter-phase mass transfer
n	density of nucleation sites
n_p	number of bubbles
Nu	Nusselt number
Pr	liquid Prandtl number
Q_c	heat transfer due to convection
Q_e	heat transfer due to evaporation
Q_{lg}	inter-phase heat transfer
Q_q	heat transfer due to quenching
Q_w	wall heat flux
Re	flow Reynolds number $= GD_h/\mu_l$
Re_b	bubble Reynolds number
St	Stanton number
T	temperature
T_{sat}	saturation temperature
U	velocity

Greek symbols

α	void fraction
k_l	liquid thermal conductivity
μ	viscosity
ρ	density
$\Delta\rho$	density difference $(\rho_l - \rho_g)$
σ	surface tension
θ	subcooling, $T_{sat} - T_l$

Subscripts

g	vapour
l	liquid
in	inlet conditions
w	wall

high pressure. Bibeau and Salcudean [12] pointed out that the rate of change in void fraction with the quality at low pressure was far more significant than at high pressures. Zeitoun and Shoukri [13] found that the void growth under the low-pressure conditions was caused by bubble size increase because larger bubbles were formed in low-pressure subcooled boiling flows, whereas bubbles tended to be very small at high pressures. Our numerical study [11] also showed that the CFX subcooled boiling model, validated for high pressures, gave unsatisfactory predictions of mean bubble size distribution in a subcooled boiling flow at low pressures.

Our first objective of this work is, therefore, to further develop the CFX boiling model so that it is capable of predicting subcooled boiling flow at low pressures. As pointed out in [14], various modelling issues need to be considered in developing accurate mechanistic models for predicting void fraction distributions in subcooled boiling flows. Zeitoun [15] presented a detailed review of these issues. The same issues were briefly summarised by Zeitoun and Shoukri [14]. As discussed below, we found that, particularly at low pressures, the most important issues were: (i) bubble size distribution and interfacial area concentration (which determines inter-phase momentum transfer and more importantly inter-phase heat transfer); (ii) partition of the wall heat flux (which determines the inter-phase mass transfer near a heated surface); and (iii) bubble departure diameter and the

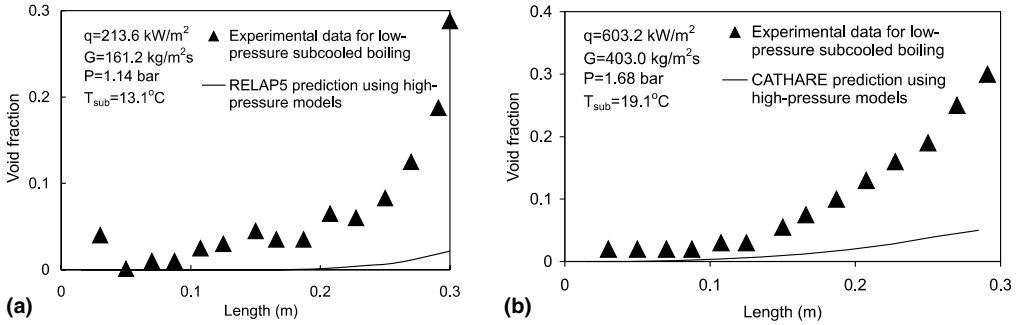

Fig. 1. Comparison of measured and predicted void fraction profiles using: (a) RELAP5; and (b) CATHARE computer code.

related bubble departure frequency (which are used to model the partition of the wall heat flux).

Also, the present study focuses on the effect of these issues or parameters on the mechanistic closure relationships and on void fraction distributions at low pressures. We found that a low-pressure bubble size correlation is essential for accurate determination of the total rate of interfacial momentum, energy and mass transport between two phases in a low-pressure subcooled boiling flow. This is because bubble size correlations commonly used for high-pressure conditions, only apply to the very small bubbles that occur at these pressures, whereas large bubbles occur in low-pressure flows. We also found that the wall heat transfer due to surface quenching, commonly not accounted for in high-pressure subcooled boiling models, was significant at low pressures because of the formation of larger bubbles before departure from the heated surface.

The second objective of this study is to compare predictions using different correlations for the above parameters with available data. Several experimental data are used to study the influence of these parameters on low-pressure void fraction distributions. By adopting several existing and new correlations, the new model from this study is validated by comparing its predictions with different types of low-pressure experimental data obtained by different groups [14,16–18].

Finally, when the present boiling model was incorporated into the RELAP5/MOD2 computer code, its prediction of void fraction distribution for low-pressure subcooled boiling flows was substantially improved. It was also found that the most significant contribution to the improvement of void prediction in the RELAP5/MOD2 code was due to the appropriate partition of the wall heat flux.

2. Subcooled boiling models

In a two-fluid mechanistic model of subcooled flow boiling, both the vapour and liquid phases are treated as continua, and two sets of conservation equations governing the balance of mass, momentum and energy of each phase are solved. A three-dimensional solution is obtained with CFX-4.2 [5], and a one-dimensional solution is obtained in RELAP5 [1]. Since the macroscopic fields of one phase are not independent of those of the other phase, models or correlations for the interaction terms that couple the transport of momentum, energy, and mass of each phase across the interfaces are required in the field equations.

As stated earlier, this paper focuses on the influence of bubble size and interfacial area concentration on the interfacial momentum and heat transport. Another focus is the effect of the partition of the wall heat flux and related parameters on interfacial mass transfer at low pressures. Three different subcooled boiling models, (1) that of the CFX-4.2 computer code [5] (here called CFX_old), (2) that of RELAP5/MOD2 computer code [1] (here called RELAP), and (3) that of the CFX-4.2 as modified as a result of the present study (called CFX_new), are evaluated in this paper. Relevant closure relationships and correlations in the above models are presented in this section. Other aspects, such as governing equations, turbulence models and other closure relationships are as discussed in the relevant literature references (e.g. [6–8]).

2.1. Inter-phase drag force and heat transfer

The total drag force per unit volume on the liquid or on the gas can be expressed as

$$F_{\mathrm{lg}}^{\mathrm{d}} = -F_{\mathrm{gl}}^{\mathrm{d}} = \frac{1}{8}\rho_{\mathrm{l}} A_{\mathrm{lg}} C_{\mathrm{D}} |U_{\mathrm{g}} - U_{\mathrm{l}}|(U_{\mathrm{g}} - U_{\mathrm{l}}), \tag{1}$$

where ρ_{l}, A_{lg}, C_{D}, and U are the liquid density, interfacial area, drag coefficient, and phasic velocity, respectively. For a bubble of a given shape, undergoing motion in a Newtonian incompressible fluid, C_{D} depends only on the bubble Reynolds number:

$$Re_{\mathrm{b}} = \frac{\rho_{\mathrm{l}}|U_{\mathrm{g}} - U_{\mathrm{l}}|d}{\mu_{\mathrm{l}}}, \tag{2}$$

where μ_{l} and d are the liquid molecular viscosity and bubble diameter. Experimental data on C_{D} as a function of Re_{b} has been correlated for several distinct Reynolds number regions for individual bubbles [19].

Heat transfer across a phase boundary is usually described in terms of an interfacial heat transfer coefficient, h_{lg}, the amount of energy in the form of heat crossing a unit area, per unit time, per unit temperature difference between two phases. The rate of heat transfer Q_{lg} per unit time across a phase boundary of area A_{lg}, is

$$Q_{\mathrm{lg}} = h_{\mathrm{lg}} A_{\mathrm{lg}} (T_{\mathrm{g}} - T_{\mathrm{l}}). \tag{3}$$

In CFX-4.2, the inter-phase heat transfer coefficient is correlated in terms of a Nusselt number, Nu, the bubble diameter d and the liquid thermal conductivity k_{l}

$$h_{\mathrm{lg}} = \frac{Nu k_{\mathrm{l}}}{d}. \tag{4}$$

For a bubble in a moving, incompressible, Newtonian fluid, the Nusselt number is a function of the bubble Reynolds number Re_{b} and the liquid phase Prandtl number $Pr = \mu_{\mathrm{l}} C_{\mathrm{pl}}/k_{\mathrm{l}}$, where C_{pl} is the liquid specific heat capacity. The Ranz and Marshall [20] Nusselt number correlation:

$$Nu = 2 + 0.6(Re_{\mathrm{b}})^{0.5} Pr^{0.3} \tag{5}$$

is used in CFX-4.2. A modified Chen correlation [21] is used in RELAP5/MOD2 for estimating the inter-phase heat transfer coefficient.

For the flow of spherical bubbles of diameter d in a liquid, CFX-4.2 and RELAP5/MOD2 estimate the interfacial area per unit volume respectively from

$$A_{lg} = \begin{cases} \dfrac{6\alpha}{d}, & \text{(CFX-4.2)}, \\ \dfrac{3.6\alpha}{d}, & \text{(RELAP5/MOD2)}, \end{cases} \tag{6}$$

where α is the void fraction. As can be seen from the above correlations, the interfacial area concentration or the mean bubble diameter is an essential parameter in determining the interfacial momentum and heat transport.

In the existing model of CFX-4.2 [5], otherwise known as CFX_old, the mean bubble diameter is modelled as a linear function of local liquid subcooling originally proposed in Anglart and Nylund [8]:

$$d = \frac{d_1(\theta - \theta_0) + d_0(\theta_1 - \theta)}{\theta_1 - \theta_0}, \tag{7}$$

where d_0 and d_1 are the bubble diameters at reference liquid subcoolings θ_0 and θ_1. Outside this subcooling range the diameters are assumed to be constant. The reference subcoolings and bubble diameters recommended by Anglart and Nylund [8] are $d_0 = 1.5 \times 10^{-4}$ m at $\theta_0 = 13.5$ K and $d_1 = 1.5 \times 10^{-3}$ m at $\theta_1 = 0$ K.

The mean bubble diameter is calculated in RELAP5/MOD2 [1] by

$$d = \frac{0.5\sigma We}{\rho_l (U_g - U_l)^2}, \tag{8}$$

where σ is the surface tension and We is the critical Weber number to be taken as 10.04 for bubbles. The mean bubble diameter is further constrained by

$$d \leqslant 0.5 D_{max}, \tag{9}$$

where D_{max} is the maximum bubble diameter calculated from

$$D_{max} = 0.0025\alpha^{1/3}. \tag{10}$$

In the present study, a low-pressure correlation for mean bubble diameter, recently proposed in [13,14], is incorporated into CFX-4.2 (here referred to as CFX_new):

$$\frac{D_s}{\sqrt{\sigma/g\Delta\rho}} = \frac{0.0683(\rho_l/\rho_g)^{1.326}}{Re^{0.324}\left(Ja + \dfrac{149.2(\rho_l/\rho_g)^{1.326}}{Bo^{0.487}Re^{1.6}}\right)}. \tag{11}$$

Here D_s is the mean Sauter bubble diameter, g the gravitational acceleration, Re the flow Reynolds number, Bo the boiling number and Ja the Jakob number based on liquid subcooling. The mean bubble diameter, d, is estimated from the mean Sauter bubble diameter, D_s.

2.2. Wall heat flux partition models

As mentioned earlier, one of the most important issues in modelling low-pressure subcooled flow boiling is the correct quantification of the partitioning of the wall heat flux at the boundary. Zeitoun [15] reviewed this topic, and found that most models divided the wall heat flux into two parts: the heat required to generate vapour; and the heat to the subcooled liquid. Bowring [22] assumed that the subcooled liquid component consisted of a single phase forced convection component together with a pumping (agitation) component predicted by a pumping factor estimated from an empirical correlation. This approach was used in most available models for predicting void fraction profile, for example, the RELAP5 computer code for high-pressure subcooled boiling flow, and was also adopted in Zeitoun and Shoukri's low-pressure subcooled boiling model [14].

However, numerous experimental and theoretical investigations for low-pressure subcooled boiling flow [23–30] suggest that there are in fact three components of the wall heat flux:

(i) heat transferred by microlayer evaporation or vapour generation, Q_e;
(ii) heat transferred by transient conduction to the superheated layer (nucleate boiling or surface quenching), Q_q; and
(iii) heat transferred by turbulent convection, Q_c.

Cooper [23], and Cooper and Lloyd [24] suggested that a low system pressure will significantly influence the growth of bubbles, promoting the formation of a liquid microlayer and forming large vapour bubbles on the heating surface. On the basis of their experimental results, Fath and Judd [25] stressed that the microlayer evaporation phenomenon was definitely a significant heat transfer mechanism at atmospheric pressure, and, depending on the heat flux, may be significant at above atmospheric pressures. This significance, however, decreases with increasing system pressure and decreasing heat flux. Recently, an experimental investigation at atmospheric pressure (Victor et al. [26]) showed that the transient conduction during the surface quenching process was the most important heat transfer mechanism, contributing up to 90 percent of the total wall heat flux. This might have been attributed to the increased quenching area resulting from the formation of large vapour bubbles and also to the subsequent enhanced degree of overlapping bubble influence area at low pressures [26].

Explanations of the mechanism for each of the heat transfer processes and formulation of empirical correlations and models were summarised by Hsu and Graham [27] and by Stephan [28]. Cooper [23] presented a theory for predicting the rate of growth of a bubble in a saturated boiling condition, allowing microlayer evaporation. Graham and Hendricks [29] formulated a

model which combines time-averaged and surface-averaged values of (i) a transient thermal conduction mechanism involving the thermal layer formed at the nucleation sites between periods of bubble nucleation; (ii) turbulent convection in regions with no bubble nucleation; and (iii) microlayer evaporation at nucleation sites while bubbles are present. Experimental verification of their model showed how these three mechanisms could adequately predict surface-averaged boiling heat fluxes. Later, Judd and Hwang [30] presented a comprehensive model for predicting the heat flux comprised of the above three components. Fath and Judd's [25] experimental data validated the model proposed by Judd and Hwang. More recently, Judd [31] studied the effect of some important parameters, such as bubble departure diameter and departure frequency, on the model prediction of boiling heat transfer.

Although the importance of these heat transfer mechanisms at low pressures has been widely stressed in literature there are few computational applications of these models. The aim of this paper is to robustly test the three-partition-wall-heat-flux model that we incorporated into the CFX computer code by comparing its predictions with experimental data, and hence to demonstrate the general feasibility of the model for predicting subcooled flow boiling at low pressures.

2.2.1. Heat transfer due to surface quenching

After a bubble departs, fresh liquid comes into contact with a heating surface. This liquid is assumed to be heated by transient conduction, with a step change in temperature at the surface. According to Mikic and Rohsenow [32], this heat flux can be predicted by the relationship

$$Q_q = \left(\frac{2}{\sqrt{\pi}}\sqrt{k_l \rho_l C_{pl}}\sqrt{f}\right) A_q (T_w - T_l), \tag{12}$$

where f is the bubble departure frequency, A_q, the fraction of wall area subjected to cooling by quenching and this is calculated by

$$A_q = nK\left(\frac{\pi d_{Bw}^2}{4}\right), \tag{13}$$

where d_{Bw} is the bubble departure diameter, n is the density of active nucleation sites and is obtained from Lemmert and Chwala's [33] correlation of data,

$$n = [210(T_w - T_{sat})]^{1.805}. \tag{14}$$

The parameter K is the ratio of the area around a nucleation site influenced by heat transported by a nucleate boiling to the projected bubble area at departure, and must be greater than the unity. A value of $K = 4$ is often recommended [34]. However, Kenning and Victor [35] found values ranging between 2 and 5. Judd and Hwang [30] found that a lower value, $K = 1.8$, best fitted their experimental data. For our modification of CFX (CFX_new), we incorporated a Jacob number dependence as suggested by Kenning and Victor [35] to be

$$K = 4.8\exp(-Ja/80). \tag{15}$$

The most important parameters in the wall heat flux partition model are the bubble departure diameter, d_{Bw}, and the bubble departure frequency, f, as pointed out in [31]. These two parameters will be discussed later.

2.2.2. Heat transfer due to evaporation

The heat flux due to vapour generation at the wall in the nucleate boiling region can be simply calculated from [22],

$$Q_e = nf\left(\frac{\pi}{6}d_{Bw}^3\right)\rho_g h_{fg}, \tag{16}$$

where h_{fg} is the latent heat. It can be seen that accurate prediction of this heat flux also depends on accurate prediction of the two important parameters mentioned above, the bubble departure diameter and the bubble departure frequency.

2.2.3. Heat transfer due to turbulent convection

The heat flux according to the definition of local Stanton number [36] for turbulent convection is

$$Q_c = St\rho_l C_{pl} U_l (T_w - T_l)(1 - A_q) \tag{17}$$

here the Stanton number is estimated by

$$St = \frac{Nu}{RePr}, \tag{18}$$

where Re is the local Reynolds number.

2.2.4. Bubble departure diameter and frequency

A number of studies have examined bubble growth and detachment at heating surfaces at low pressures [37–40]. Other recent empirical correlations for bubble departure diameter and frequency, for example, Rodgers et al. [37], Judd [31], Zeng et al. [38] and Rodgers and Li [39], were not evaluated in the present study. For bubble departure diameter, the correlation of Unal [40] is adopted for CFX_new

$$d_{Bw} = \frac{2.42\times 10^{-5} p^{0.709} a}{\sqrt{b\Phi}}, \tag{19}$$

where

$$a = \frac{(q_w - h_l\theta)^{1/3} k_l}{2C^{1/3} h_{fg}\sqrt{\pi k_l/\rho_l c_{pl}}\rho_g}\sqrt{\frac{k_w \rho_w c_{pw}}{k_l \rho_l c_{pl}}},$$

$$C = \frac{h_{fg}\mu_l[c_{pl}/(0.013 h_{fg} Pr^{1.7})]^3}{[\sigma/(\rho_l - \rho_g)g]^{0.5}},$$

$$b = \theta/2(1 - \rho_g/\rho_l)$$

$$\Phi = \begin{cases} \left(\frac{u_l}{0.61}\right)^{0.47} & \text{for } u_l \geqslant 0.61 \text{ m/s}, \\ 1.0 & \text{for } u_l < 0.61 \text{ m/s}. \end{cases}$$

The stated range of this correlation is

Pressure	$0.1 < p < 17.7$ MPa
Wall heat flux	$0.47 < q_w < 10.64$ MW/m^2
Liquid velocity	$0.08 < u_l < 9.15$ m/s
Liquid subcooling	$3.0 < \theta < 86$ °C

For comparison purposes, we used two other bubble departure diameter correlations: the equation proposed by Fritz [41] for low pressure

$$d_{Bw} = 0.208\varphi\sqrt{\frac{\sigma}{g(\rho_l - \rho_g)}}, \tag{20}$$

where φ is the contact angle, to be taken as 80° according to [39], and the empirical correlation of Tolubinskiy and Kostanchuk [42] (inbuilt into CFX_old)

$$d_{Bw} = \min[0.0006\exp(-\theta/45), 0.0014]. \tag{21}$$

For the relationship between bubble departure frequency and bubble departure diameter, we incorporated the equation proposed by Cole [43] for the low-pressure condition into CFX (CFX_new)

$$f = \sqrt{\frac{4g(\rho_l - \rho_g)}{3d_{Bw}\rho_l}}. \tag{22}$$

For comparison purposes, we also considered another two correlations: that of Ivey [44]

$$f = 0.9\sqrt{\frac{g}{d_{Bw}}}, \tag{23}$$

and that of Stephan [28]

$$f = \frac{1}{\pi}\sqrt{\frac{g}{2d_{Bw}}}\left[1 + \frac{4\sigma}{d_{Bw}^2\rho g}\right]^{0.5}. \tag{24}$$

2.2.5. Algorithm for calculating heat flux partitions

The total heat flux at the wall, Q_w, partitioned into three components, must satisfy

$$Q_w = Q_q + Q_e + Q_c. \tag{25}$$

Each component on the right-hand side of this equation is modelled as described above. A bisection algorithm, an iterative procedure, is employed to evaluate a wall temperature that satisfies Eq. (25). This algorithm starts with a guess of the wall temperature, and then calculates each component of the heat flux. The difference between the computed total heat flux and the actual applied wall heat flux provides a basis for a new wall temperature estimate for the next step in the iterative procedure. The iteration continues until the difference error between the applied and calculated wall heat flux is less than a prescribed fraction (here $<10^{-4}$) of the applied heat flux.

2.3. Inter-phase mass transfer

Inter-phase mass transfer results from the combined effects of evaporation at the wall and of bulk condensation or evaporation. The mass transfer from liquid to vapour at the wall due to evaporation comes directly from the heat transfer due to evaporation

$$m_{wg} = \frac{Q_e}{h_{fg} + C_{pl}\theta}. \tag{26}$$

In the interior of the flow, the mass transfer rate between the two phases depends upon the liquid temperature. When the liquid is subcooled, there is bulk condensation from the gas phase to the liquid. When the liquid is super-heated, there is bulk evaporation from the liquid to the gas. Both these rates depend on the interphase heat transfer rate and the latent heat. For condensation, the mass transfer rate from gas to liquid is

$$m_{gl} = \max\left(\frac{h_{lg}A_{lg}(T_{sat} - T_l)}{h_{fg}}, 0\right). \tag{27}$$

For evaporation the mass transfer rate from liquid to gas is

$$m_{lg} = \max\left(\frac{h_{lg}A_{lg}(T_l - T_{sat})}{h_{fg}}, 0\right). \tag{28}$$

3. Results

Experimental data covering a range of heat flux, subcooling and flow conditions at low pressures have been selected for examining the numerical models and for comparing predictions obtained with these numerical models. The experimental conditions of the selected data are listed in Table 1.

All these experimental data were obtained using the gamma attenuation technique in different channel geometries and for subcooled boiling flow at low pressures (1–2 bar). The data of Zeitoun and Shoukri [14], and of Donevski and Shoukri [17] were obtained for a vertical 306 mm long concentric annular test section with an outer diameter of 25.4 mm and an inner diameter of 12.7 mm. Dimmick and Selander's [16] data was obtained for subcooled flow boiling inside a tube of 12.29 mm inside diameter. The data of Evangelisti and Lupoli [18] was obtained at atmospheric pressure in a vertical 500 mm long annular channel of 13 mm outer diameter and 7 mm inner diameter.

Table 1
Examined conditions

References	Case No.	q (kW/m^2)	G (kg/m^2 s)	P (bar)	θ_{in} (°C)	U_{in} (m/s)
[14]	1	286.68	156.15	1.37	14.9	0.164
	2	705.50	411.70	1.5	22.5	0.433
[16]	3	1160.0	634.5	1.65	61.0	0.670
	4	1164.0	1115.0	1.65	38.0	1.180
[17]	5	481.4	392.1	1.54	18.5	0.413
	6	576.1	429.0	1.68	19.5	0.453
[18]	7	437.0	1413.0	1.13	17.0	1.479

3.1. Comparison of bubble size and interfacial area distribution

The experimental data of Zeitoun and Shoukri [14] (here, cases 1 and 2) have been used to examine the effect of various parameters and models on the numerical prediction. Fig. 2 compares the measured and predicted values of void fraction profile along the heated section using three models examined in this paper. CFX_old and RELAP have both considerably underpredicted these low pressure void fraction data.

Fig. 3 compares measured and predicted bubble diameters normalised by the length scale $\sqrt{\sigma/g\Delta\rho}$ along the heated section. It can be seen from this figure that the RELAP model consistently underpredicts bubble sizes by an unacceptable margin. This underprediction at low pressures arises from the application of models developed and evaluated only for high-pressure conditions.

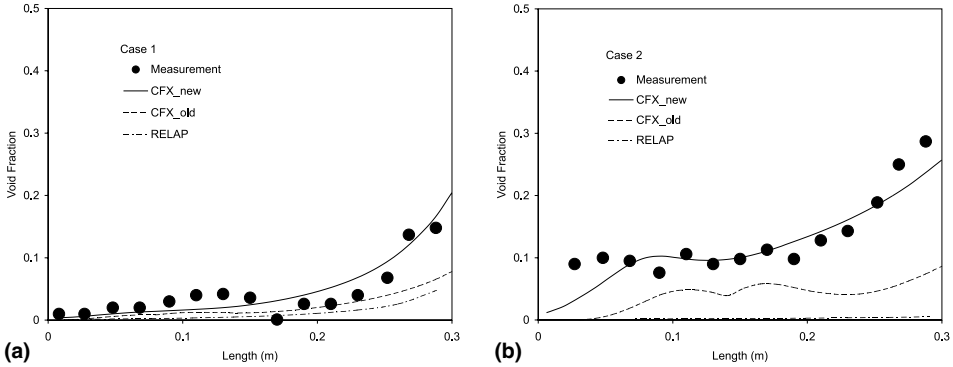

Fig. 2. Comparison of predicted void fraction profiles with experimental data.

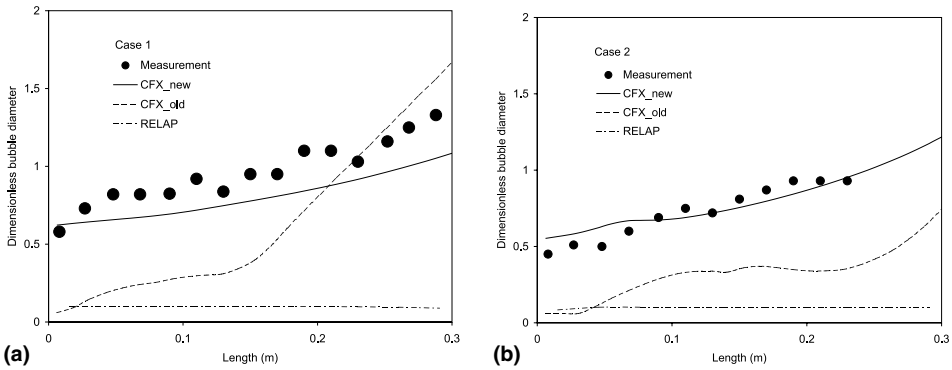

Fig. 3. Comparison of measured and predicted bubble size distribution.

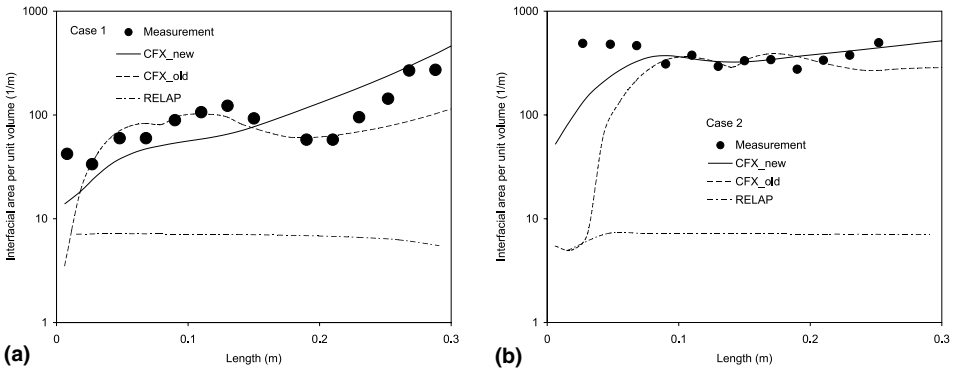

Fig. 4. Comparison of measured and predicted interfacial area profiles.

Fig. 4 compares interfacial area concentration profiles predicted using Eq. (6) with measured values. RELAP also under-predicts interfacial area concentration distribution. This is a consequence of its underprediction of the void fraction (see Fig. 2).

3.2. Comparison of heat transfer predictions

The wall heat partitions and interfacial heat transfer as predicted by the CFX_new and CFX_old models are compared here. Because the RELAP wall heat partition

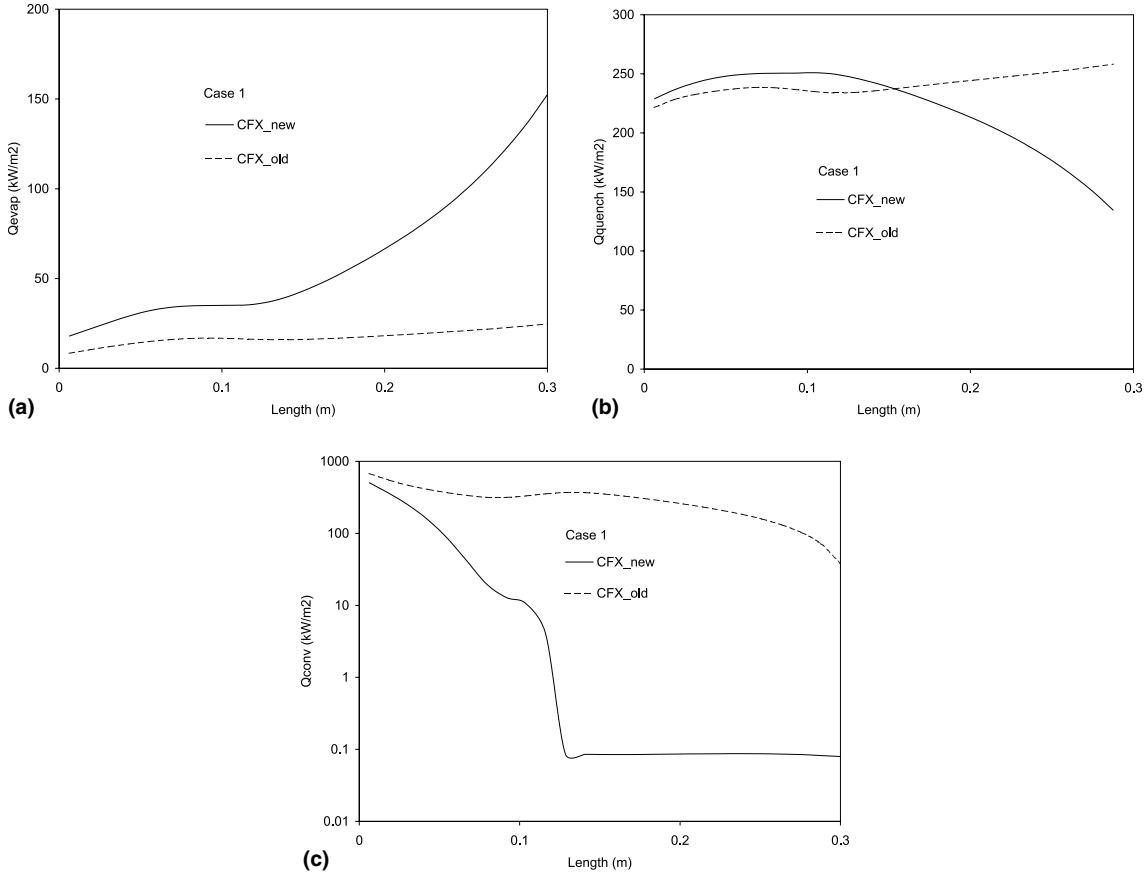

Fig. 5. Comparison of predicted wall heat flux partitions due to: (a) evaporation; (b) surface quenching; and (c) turbulent convection for Case 1.

model does not include surface quenching, the RELAP model results are not considered here.

The three heat transfer components of the total wall heat flux are evaporation, surface quenching, and turbulent convection. It should be noted that only the evaporation component contributes to vapour generation and void fraction. Fig. 5 shows CFX_new and CFX_old predictions for the above three components for Case 1. Before the onset of significant net vapour generation (ONVG, at about 0.1 m length in Case 1),

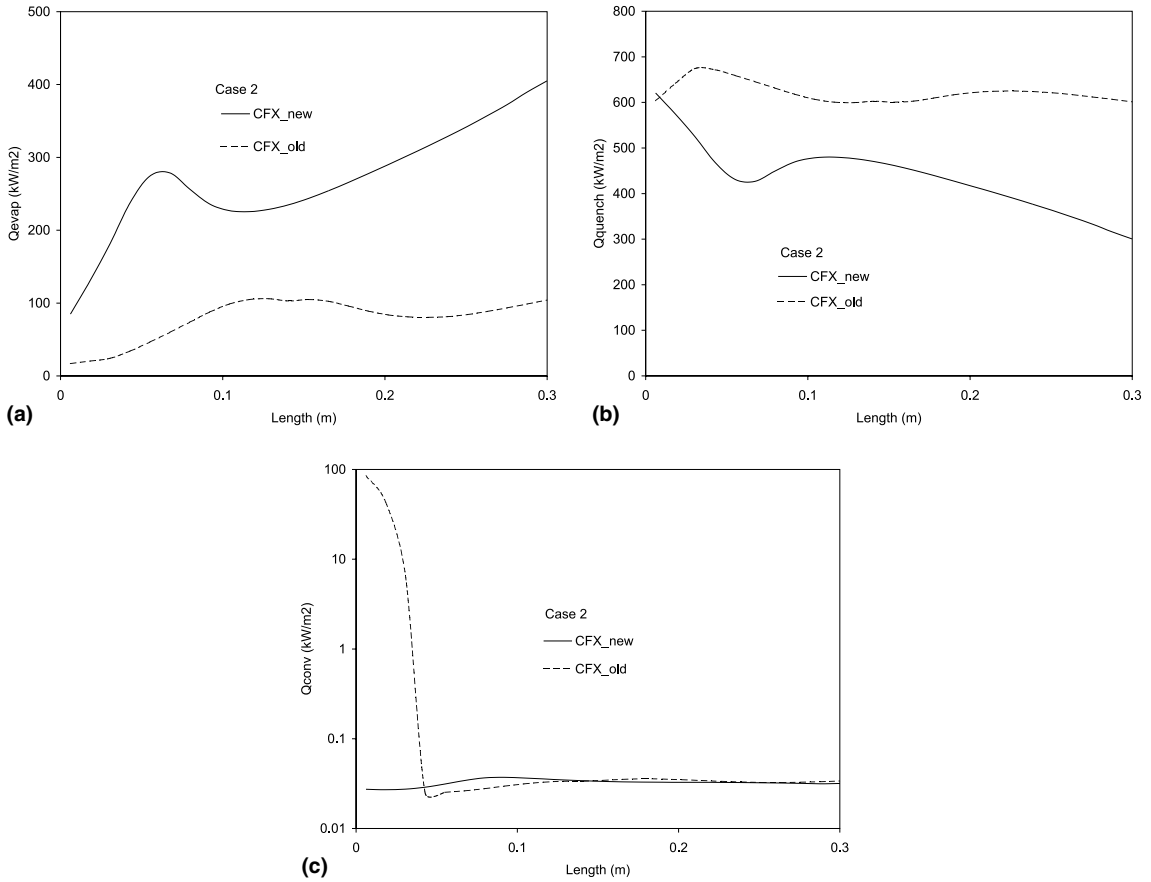

Fig. 6. Comparison of predicted wall heat flux partitions due to: (a) evaporation; (b) surface quenching; and (c) turbulent convection for Case 2.

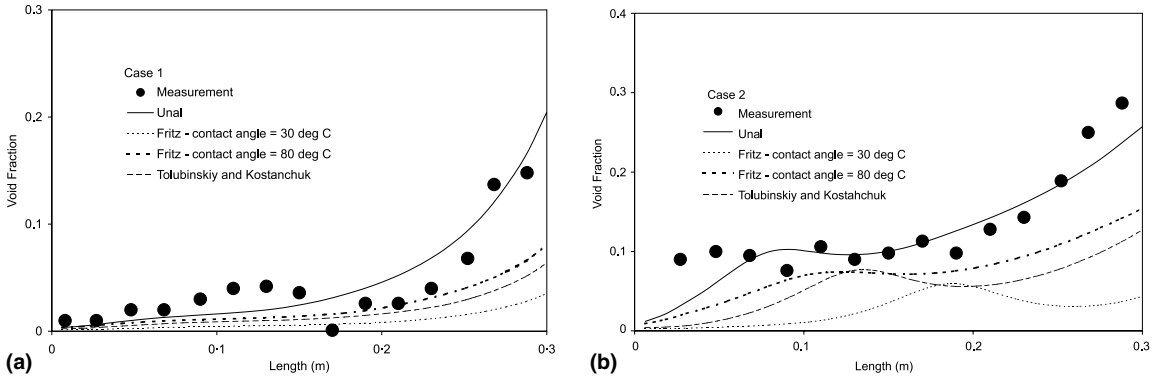

Fig. 7. Comparison of predicted void fraction using different correlations for bubble departure diameter.

CFX_new predicts that turbulent convection and surface quenching are the main causes of wall heat removal. After ONVG, turbulent convection heat transfer rapidly decreases to a negligible level, and heat transfer, due to surface quenching, also gradually decreases. At the same time evaporative heat transfer starts to increase with a similar trend to void fraction (see Fig. 2).

However, both before and after ONVG, CFX_old consistently predicts higher contributions to heat transfer from turbulent convection and surface quenching.

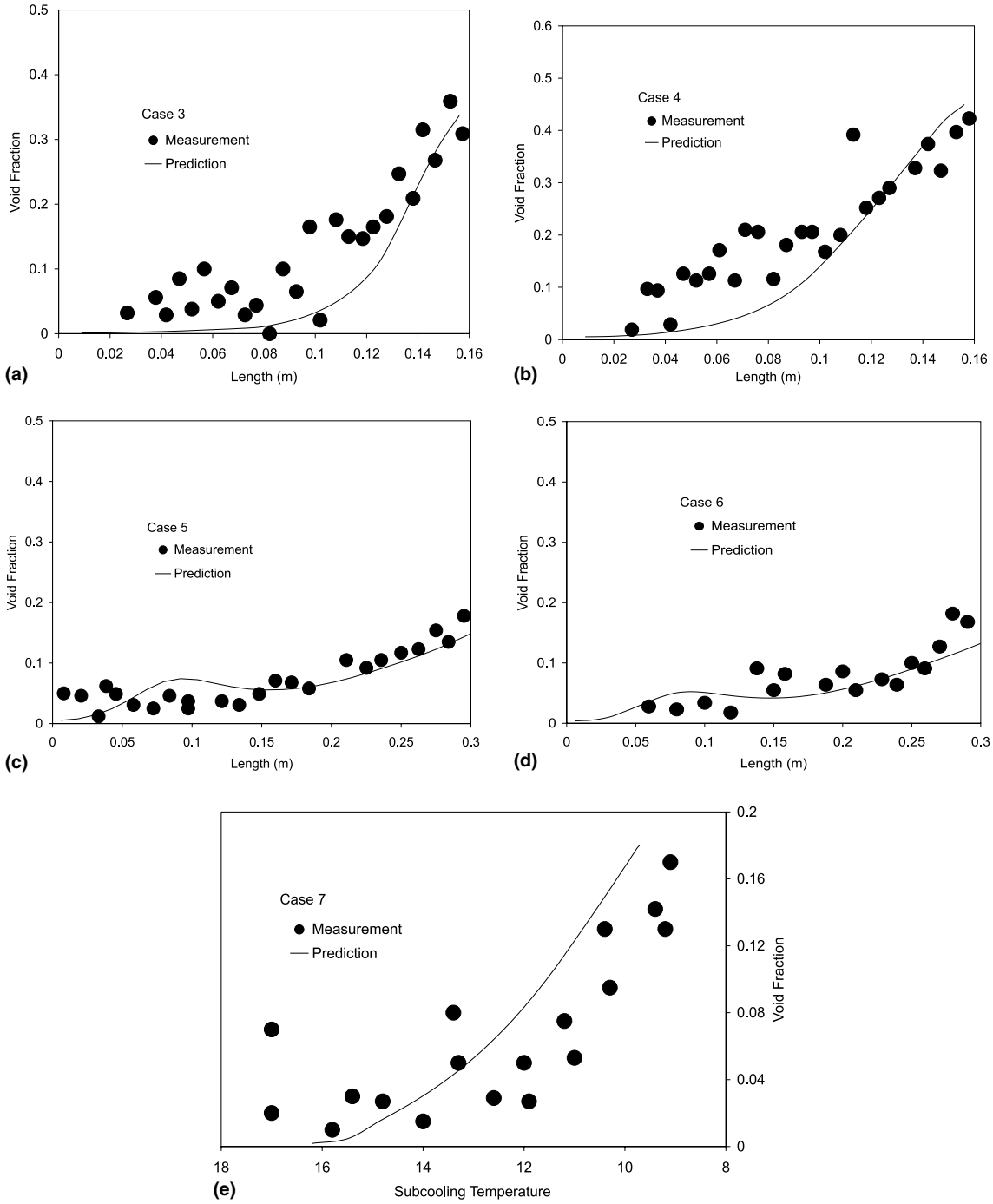

Fig. 8. Comparison of measured and predicted void fraction for Cases 3–7.

Since the total heat transfer from the wall remains unaffected, the predicted evaporative heat transfer, which contributes to vapour generation is correspondingly low. It may be concluded that evaporative heat transfer is underpredicted by the CFX_old model as a result of over-prediction of the other heat transfer components of the wall heat flux.

The predicted partitioning of wall heat flux for Case 2 is as shown in Fig. 6. In this case, the contribution to heat removal by turbulent convection is negligible, when compared with other heat transfer components. CFX_new's predicted surface quenching component of heat transfer decreases monotonically towards the exit of the heated section. As a result, the predicted contribution to heat transfer from evaporation increases with the same trend shown by the void fraction increase along the heated section. This confirms the strong link between the evaporation component of wall heat flux and void fraction. As with the conditions of Case 1, CFX_old also under-predicts void fraction in Case 2 because it under-predicts the evaporation component of heat transfer and over-predicts the surface quenching component of heat transfer.

We also tested other correlations for bubble departure diameter and frequency used for modelling wall heat partitions. It was found that there was almost no difference for the prediction of void fraction by applying the different correlations (Eqs. (22)–(24)) for bubble departure frequency while the correlation for bubble departure diameter we used in CFX_new predict void fractions better (see Fig. 7).

3.3. Comparison of predicted void fraction with other low-pressure data

Predicted void fractions have been compared with the experimental data of Zeitoun and Shoukri [14] in Fig. 2. As can be seen, the CFX_new's predictions agree closely with the data. However, this may turn out as expected, since the model within CFX_new includes a mean bubble diameter correlation based on Zeitoun and Shoukri's [13,14] experimental data. To test whether the model of CFX_new applies more generally at low pressures, predictions from CFX_new were compared with, different types of available experimental data from literature covering a range of flow conditions, heat flux, flow rate, subcooling at inlet and pressure (less than 2 bar), and geometries (annular channels and tubes), as listed in Table 1. Of specific interest for research reactor applications is its validity for high-heat flux and high-flow rate subcooled boiling flows. ANSTO's HIFAR research reactor operates at a peak heat flux of about 800 kW/m^2 and a flow rate of approximately 3000 kg/m^2 s. Thus, the high-heat flux (to 1160 kW/m^2) and high-flow rate (to 1400 kg/m^2 s) data of the literature are specifically targeted for comparison.

Fig. 8 compares predicted void fractions obtained from CFX-new with the above-mentioned data. As can be seen, the agreement between the predictions using the present model and the experimental void fractions is generally very good.

3.4. Comparison of predicted void fraction using REALP5 with low-pressure data

In order to confirm our understanding and observation from the above study, we have carried out a systematic test, using the RELAP5 code, of the various parameters that control the void fraction generation in *low-pressure* subcooled boiling flows. We found that the correct quantification of the wall heat partitions for the boiling model in the RELAP5 code is the determining mechanism for good void fraction prediction. When the present model includes the partitioning of wall heat flux, mean bubble diameter, and interfacial heat transfer into the RELAP5/MOD2 computer code (RELAP5/MOD2-new), its capacity to predict void fractions in low-pressure subcooled boiling flows improves substantially.

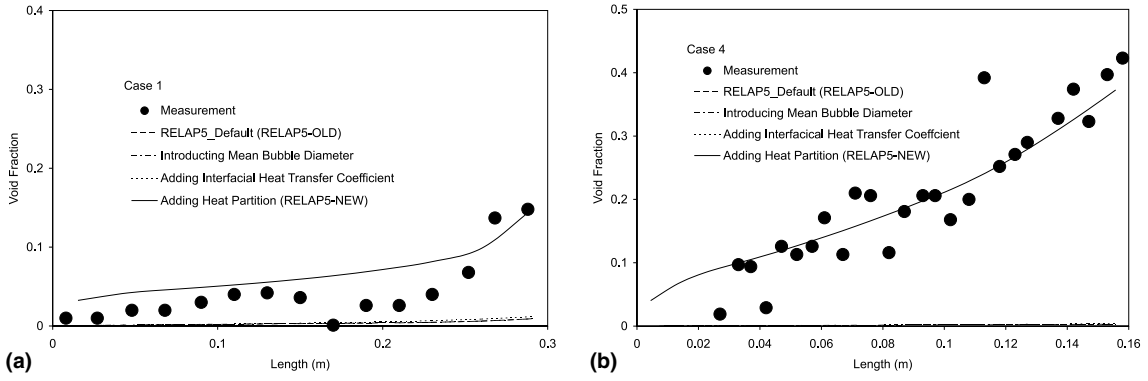

Fig. 9. Comparison of measured and predicted void fraction profiles using RELAP5_OLD and RELAP5_NEW models.

This is clearly demonstrated in Fig. 9. Further validation of RELAP5_new model with a wide range of experimental data is currently under way and the results will be reported elsewhere.

4. Conclusions

Many available models developed for high-pressure subcooled boiling flow are ineffective at low pressures. A subcooled boiling model, previously validated for high pressure in the CFX-4.2 code, has been modified so that it also accurately predicts void fraction in low-pressure subcooled boiling flows. Important modelling issues and parameters for subcooled flow boiling at low pressure are the partitioning of the wall heat flux; mean bubble diameter; and bubble departure diameter. Modelling of these parameters, as presented here, has been examined for subcooled flow boiling at low pressure by comparing predictions from the modelling with a wide range of experimental data. Agreement is generally very good. When the present boiling model is introduced into the RELAP5/MOD2 computer code, its prediction of void fraction distribution in low-pressure subcooled boiling flow is also substantially improved. This confirms our understanding and observation about the important issues or parameters for accurately predicting low-pressure boiling flows.

References

[1] RELAP5/MOD2 Code Manual, NUREG/CR-5273, 1989.
[2] CATHARE 2 code, CATHRE Fifth International Seminar, CEA-DRN, 1997.
[3] S. Hari, Y.A. Hassan, J.Y. Tu, Simulation of a subcooled boiling experiment using RELAP5/MOD3.2 computer code, in: Proceedings of the ASME Nuclear Engineering Division, NE-Vol. 22, 1998, pp. 45–47.
[4] W.L. Woodruff, N.A. Hanan, J.E. Matos, A comparison of the RELAP3/MOD3 and PAET/ANL codes with the experimental transient data from the SPERT-IV D-12/25 series, Technical Report of Argonne National Laboratory, Argonne, 1997.
[5] CFX-4.2 Solver Manual, CFX, AEA Technology, Didcot, Oxon, UK, 1997.
[6] M. Kurul, Multidimensional effects in two-phase flow including phase change, Ph.D. Thesis, Rensselaer Polytechnic Institute, 1990.
[7] H. Anglart, Modelling of vapour generation at wall in subcooled boiling two-phase flow, in: First CFDS International User Conference, Oxford, UK, 1993, pp. 183–207.
[8] H. Anglart, O. Nylund, CFD application to prediction of void distribution in two-phase bubbly flows in rod bundles, Nucl. Sci. Eng. 163 (1996) 81–98.
[9] J. Mi, D.J. Burt, H. Pordal, Two-phase modelling of vapor generation in a uniformly heated vertical channel, Unpublished Technical Report, AEA Technology Engineering Software, 1998.
[10] G.G. Bartolomei, V.G. Brantov, Y.S. Molochnikov, An experimental investigation of true volumetric vapour content with subcooled boiling in tubes, Thermal Eng. 29 (3) (1982) 132–135.
[11] J.Y. Tu, The influence of bubble size on void fraction distribution in subcooled flow boiling at low pressure, Int. Commun. Heat Mass Transfer 26 (1999) 607–616.
[12] E.L. Bibeau, M. Salcudean, A study of bubble ebullition in forced convective subcooled nucleate boiling at low pressure, Int. J. Heat Mass Transfer 37 (1994) 2245–2259.
[13] O. Zeitoun, M. Shoukri, Bubble behavior and mean diameter in subcooled flow boiling, ASME J. Heat Transfer 118 (1996) 110–116.
[14] O. Zeitoun, M. Shoukri, Axial void fraction profile in low pressure subcooled flow boiling, Int. J. Heat Mass Transfer 40 (1997) 867–879.
[15] O. Zeitoun, Subcooled flow boiling and condensation, Ph.D. Thesis, McMaster University, Hamilton, ON, 1994.
[16] G.R. Dimmick, W.N. Selander, A dynamic model for predicting subcooled void: experimental results and model development, EUROTHERM Seminar #16, Pisa, Italy, 1990.
[17] B. Donevski, M. Shoukri, Experimental study of subcooled flow boiling and condensation in an annular channel, Thermofluids Report No. ME/89/TF/R1, Department of Mechanical Engineering, McMaster University, Hamilton, ON, 1989.
[18] R. Evangelisti, P. Lupoli, The void fraction in an annular channel at atmospheric pressure, Int. J. Heat Mass Transfer 12 (1969) 699–711.
[19] M. Ishii, N. Zuber, Drag coefficient and relative velocity in bubbly, droplet or particulate flows, AIChE J. 25 (1979) 843–855.
[20] W.E. Ranz, W.R. Marshall, Chem. Eng. Prog. 48 (1952) 141–148.
[21] J.C. Chen, A correlation for boiling heat transfer too saturated fluid is in can working flow, Process Des. Dev. 5 (1966) 322–327.
[22] R.W. Bowring, Physical model based on bubble detachment and calculation of steam voidage in the subcooled region of a heated channel, Report HPR-10, Institute for Atomenergi, Halden, Norway, 1962.
[23] M.G. Cooper, The microlayer and bubble growth in nucleate pool boiling, Int. J. Heat Mass Transfer 12 (1969) 915–933.
[24] M.G. Cooper, A.J.P. Lloyd, The microlayer in nucleate pool boiling, Int. J. Heat Mass Transfer 12 (1969) 895–913.
[25] H.S. Fath, R.L. Judd, Influence of system pressure on microlayer evaporation heat transfer, ASME J. Heat Transfer 100 (1978) 49–55.
[26] H. Victor, M. Del Valle, D.B.R. Kenning, Subcooled flow boiling at high heat flux, Int. J. Heat Mass Transfer 28 (1985) 1907–1920.
[27] Y.Y. Hsu, R.W. Graham, Transport Processes in Boiling and Two-phase Systems, Hemisphere, Washington, DC, 1976.
[28] K. Stephan, Heat Transfer in Condensation and Boiling, Springer, New York, 1992.
[29] R.W. Graham, R.C. Hendricks, Assessment of convection and evaporation in nucleate boiling, NASA TN D-3943, 1967.

[30] R.L. Judd, K.S. Hwang, A comprehensive model for nucleate pool boiling heat transfer including microlayer evaporation, ASME J. Heat Transfer 98 (1976) 623–629.
[31] R.L. Judd, The role of bubble waiting time in steady nucleate boiling, ASME J. Heat Transfer 121 (1999) 852–855.
[32] B.B. Mikic, W.M. Rohsenow, A new correlation of pool walking data including the fact of heating surface characteristics, ASME J. Heat Transfer 91 (1969) 245–250.
[33] M. Lemmert, J.M. Chwala, Influence of flow velocity on surface boiling heat transfer coefficient, in: E. Hahne, U. Grigull (Eds.), Heat Transfer in Boiling, Academic Press and Hemisphere, New York and Washington, DC, 1977.
[34] C.Y. Han, P. Griffith, The mechanisms of heat transfer in nucleate boiling the heat flux temperature difference relationship, Int. J. Heat Mass Transfer 8 (1965) 905–914.
[35] D.B.R. Kenning, H. Victor, M. DelValle, Full developed nucleate boiling: overlap of areas of influence and interference between bubble sites, Int. J. Heat Mass Transfer 24 (1981) 1025–1032.
[36] A. Bejan, Heat Transfer, Wiley, New York, 1993, p. 260.
[37] J.T. Rogers, M. Salcudean, Z. Abdullah, D. McLeod, D. Poirier, The onset of significant void in up-flow boiling of water at low pressure and velocities, Int. J. Heat Mass Transfer 30 (1987) 2247–2260.
[38] L.Z. Zeng, J.F. Klausner, R. Mei, A unified model for the prediction of bubble detachment diameters in boiling systems – I. Pool boiling, Int. J. Heat Mass Transfer 36 (1993) 2261–2270.
[39] J.T. Rogers, J. Li, Prediction of the onset of significant void in flow boiling of water, ASME J. Heat Transfer 116 (1994) 1049–1053.
[40] H.C. Unal, Maximum bubble diameter, maximum bubble growth time and bubble growth rate, Int. J. Heat Mass Transfer 19 (1976) 643–649.
[41] W. Fritz, Berechnung des Maximalvolumes von Dampfblasen, Phys. Z. 36 (1935) 379.
[42] V.I. Tolubinsky, D.M. Kostanchuk, Vapour bubbles growth rate and heat transfer intensity at subcooled water boiling, in: Fourth International Heat Transfer Conference, 5, Paper No. B-2.8, Paris, 1970.
[43] R. Cole, A of photographic study of pool boiling in the region of the critical heat flux, AIChE J. 6 (1960) 533–542.
[44] H.J. Ivey, Relationships between bubble frequency, departure diameter and rise velocity in nucleate boiling, Int. J. Heat Mass Transfer 10 (1967) 1023–1040.